Dislocation theory of dimer melting in two dimensions: Lipid membranes

A. Holz and D. T. Vigren
Universität des Saarlandes, D-6600 Saarbrücken, West Germany

M. Zuckermann
McGill University, Montreal, Quebec, Canada H3A 2T8

(Received 12 March 1984)

A dislocation theory of dimer melting in two dimensions is presented in which the solid state is considered as a random array of close-packed dimers on a triangular lattice. Possible application of the model to phospholipid bilayer membranes is discussed, and comparison with the melting of two-dimensional monatomic systems, as well as of layered paraffins, is made.

I. INTRODUCTION

The phase behavior of pure phospholipid bilayers has been the subject of considerable investigation, both theoretical and experimental.[1–9] The chemical structure of a typical phospholipid molecule (DPPC) is shown in Fig. 1(a). It consists of two hydrocarbon chains (R), which range in length from 12 to 22 CH_2 units, joined together by a glyceride "backbone" at one end, and topped by a polar head with the chemical group $C-O-(PO_3)^- X$. Owing to the hydrophilic quality of the choline subunit X, as well as the hydrophobic nature of the CH_2 chains, the molecules of the lipid membrane orient, as shown in Fig. 1(b), in the solid state. The chains may be perpendicular or at a tilt to the membrane surface and the aqueous medium above it.

Hydrated lipid multibilayers exhibit a variety of phase transitions, which include a solid-liquid transition at T_M' (the main "gel"—to—liquid-crystal transition), and structural transitions within the crystalline gel phase, such as the sub-transitions and pretransitions. Within the gel phase the hydrocarbon chains are thought to be rather rigid with the glyceride backbones forming a close-packed triangular structure within the membrane surfaces. Within these surfaces the backbone axes are rotationally disordered with respect to each other so as to preserve the triangular symmetry, as shown in Fig. 1(c).

At T_M' two events occur *simultaneously*: (i) The two-dimensional lattice melts into a dense fluid, and (ii) the hydrocarbon chains become internally disordered through transgauche isomerization ("chain melting"). This latter effect causes a decrease in the thickness of the bilayer, although the bilayer itself seems to persist above T_M', making the high-temperature phase somewhat analogous to the smectic A phase of some liquid crystals.

It is supposed, at least for the longer-chain homologs, that the dominant contribution to the transition enthalpy derives from chain melting. For this reason considerable theoretical effort has been devoted to calculating the statistical mechanics of chain conformations. In this paper we address ourselves to the following questions: How can the constraint of chain pairing on a triangular lattice, especially pronounced near the lipid membrane surfaces, be incorporated into a theory of dislocation-mediated melting of quasi-two-dimensional systems, as developed, for example, in the treatment of paraffin? Furthermore, does such a theory explain the melting transition as one which leads the system into a liquid-crystal phase above T_M'?

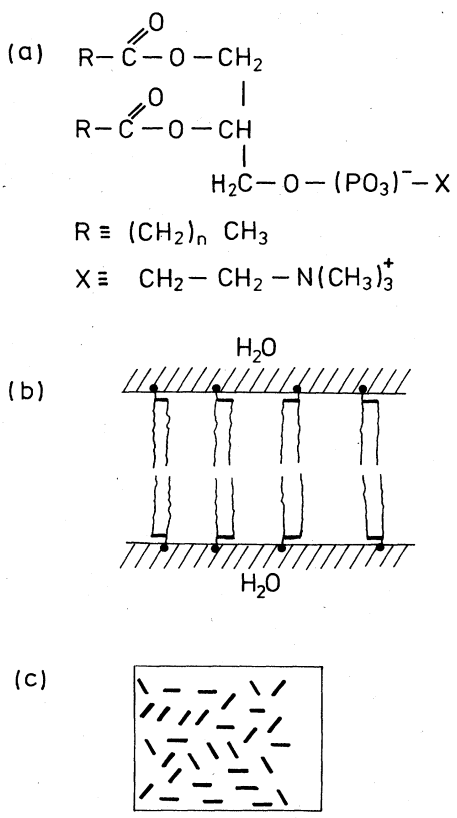

FIG. 1. Schematic representation of phospholipid bilayer in low-temperature gel phase. (a) Chemical formula of DPPC, a typical lipid molecule. (b) Side view of membrane: ⁞, polar head; —, glyceride backbone; ~~ hydrocarbon chain. (c) top view of membrane: glyceride backbones are arranged at random on a triangular lattice.

To this end we consider the detailed mechanisms involved in the melting of a two-dimensional dimer solid at T_M, which may be construed as representing a lipid monolayer with perfectly rigid CH_2 chains. In fact, this limit may be important when the CH_2 chains are very short, or at high lateral pressures, where interchain interactions are expected to suppress the lateral degrees of freedom of the chains.

In Sec. II we present a detailed discussion of dislocation pair dissociation in the dimer solid, paying particular attention to the steric constraints on slip motion, and those processes by which the barriers to slippage may be overcome. Here the principal mechanisms are thought to be cooperative rotational fluctuations and/or the creation of additional dislocation pairs, which may assume various configurations in the wake of an advancing slip line.

In Sec. III we consider in detail nonconservative processes of barrier unlocking through intermediate-pair production. We show that five basic processes of barrier removal exist, and proceed to ennumerate the various remnant pair configurations associated with them. Owing to the detailed nature of the descriptions presented here, we suggest that the reader gloss briefly over this section in a first reading.

In Sec. IV a dislocation theory of melting is presented in which the mutual interactions of the intermediate pairs associated with the slip line of a given widely separated reference pair, are approximated by a screening (or antiscreening) of the reference-pair interaction. Here upper-bound melting temperatures, T_M^{**} and T_M^{*}, are obtained for the dimer solid with and without intermediate-pair excitations, respectively.

In Sec. V we describe a numerical calculation of the mutual interaction energy of the dislocations involved in randomly generated slips. The interaction energy of paths of equal length are averaged over a limited ensemble of 30 paths of given length. The results are then used to suggest a correction to the expression for T_M^{*} obtained in Sec. IV.

In Sec. VI the results of the model are discussed and compared with well-known qualitative limits of monatomic chain melting of two-dimensional lattices. In Sec. VII possible extensions of the dislocation melting theory to account for chain flexibility are discussed. In particular, the similarity of the present system with that of paraffin homologs is analyzed,[10] and possible extensions of the melting theory of paraffins to that of lipid membranes are proposed. Furthermore, the general significance of the results obtained is discussed.

II. DISLOCATIONS AND SLIP IN THE DIMER SOLID

A. General discussion

In a dislocation theory of *monatomic* melting in two dimensions, point dislocations, which exist mainly in tightly bound pairs in the solid, become dissociated at the melting temperature T_M.[11–13] The dissociation is facilitated because *thermally produced* tightly bound dislocation dipoles screen out the elastic interaction between the elements of a given widely separated reference pair.

In the dimer solid, however, a given thermally produced pair is not free to separate through the production of a straight slip line between its constituents. In fact, the steric constraint of dimer pairing of the lattice points impedes the slip. To see this we consider a completely ordered dimer solid as shown in Fig. 2. In Fig. 2(a) the slip line (dashed line) lies between the two rows of dimers shown, so that the upper rows of molecules can slip one lattice spacing to the left or right, relative to the lower row, whereas in Fig. 2(b) the slip line cuts through the lower row of dimers, so that the upper row of endpoints can slip one lattice spacing to the left, relative to the lower row, *but not* to the right (the allowed slip, being affected through a counterclockwise rotation of the molecules in their plane).

In application to the lipid membrane problem we wish to consider the dimers to be rotationally disordered with respect to one another in their common plane, while maintaining the triangular symmetry in the solid state. To sustain such a state of disorder dynamically, if one does not consider the dimers to be frozen in, requires a cooperative rotational flipping motion of the dimers over rather large clusters, in such a manner that the triangular symmetry in a time average is globally preserved. Since these coherent flipping motions may, in general, be viewed as density fluctuations followed by the creation and annihilation of tightly bound dislocation pairs with zero resultant strength, one expects them to be thermally activated processes. Although the counting problem of dimers on a lattice has been solved, their statistical mechanics, incorporating transitions over activation barriers, remains to be studied. Because the ground state of the dimer system is infinitely degenerate it must be either a frozen-in state or a dynamically disordered one. In this paper we assume that the latter prevails.

Assuming that slip motion proceeds more rapidly than the activated, cooperative rotational fluctuations, the slip is most likely terminated after some lattice spacings $\langle n \rangle$

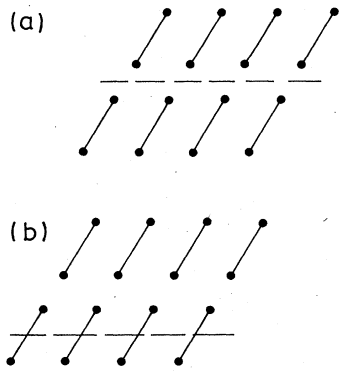

FIG. 2. Two possible slip lines (dashed lines) in a completely ordered dimer solid.

by a dimer which is unable to move in the appropriate direction. We refer to such dimers as "blocking dimers." To estimate $\langle n \rangle$ one notes that the probability that a dimer does not impede slippage is $p=\frac{5}{6}$ and that it blocks slippage, $q=\frac{1}{6}$, so that the probability of a slip segment n spacings in length is $P(n)=p^n q$, and

$$\langle n \rangle \equiv \sum_{n=1}^{\infty} nP(n)=pq(1-p)^{-2}=5 .$$

B. Conservative rotational processes

Once a blocking dimer has impeded the progress of a dislocation, the barrier may be overcome by simply waiting until a barrier-"unlocking" fluctuation rotates the blocking dimer to a new position that is favorable to slip. In Fig. 3 we have sketched some dimer configurations which block the circled dislocation. We term such clusters (n,m) locks since the barrier to dislocation motion imposed by the blocking dimers may be "unlocked" through n counterclockwise and m clockwise rotational flips of those dimers participating in the lock. It should be noted that such correlated flips are necessarily accompanied by local-density and/or slip fluctuations in order that the steric constraints of the lock may be relieved so as to allow the flips. These fluctuations must be thermally activated and hence must be specified for a complete characterization of the lock. Therefore the partial specification (n,m) will be termed the "signature" of the lock.

Figure 3(a) illustrates the opening of a (2,0) lock. The initial positions of the dimers in the lock are characterized by ellipses labeled i; the final, unlocked positions are labeled f. Obviously, steric constraints forbid the rotations of $\pi/3$, as indicated in the figure by arrows, without a local fluctuation, in this case represented by a dislocation dipole of core separation $2\vec{b}$, as shown. Here, $\pm\vec{b}$ are the Burgers vectors of the constituents of the dipole. After the $\pi/3$ rotations the dimers relax to their final positions through a local compression. Since the dipole pair may annihilate at the end of this process, it is a conservative process.

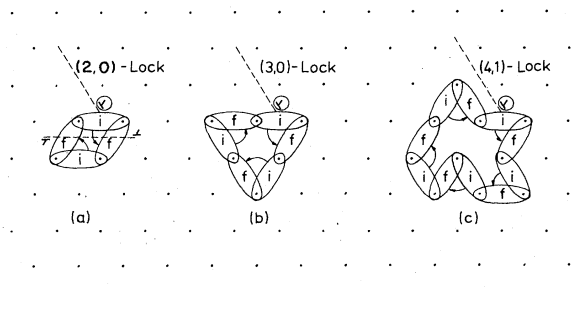

FIG. 3. Dimer clusters which present barriers to the motion of the circled dislocations. The dimers in initial (i) and final (f) positions are represented as solid ellipses. Arrows indicate the sense of rotation so as to "open the lock." The signature (n, m) of the lock indicates the number of (counterclockwise, clockwise) rotations involved. The activated fluctuations associated with these motions are explained in the text.

Once the lock opens, the impeded dislocation may proceed in the forward direction until it is again blocked. In Figs. 3(b) and 3(c), locks of higher order are shown which involve three and five dimers, respectively. The (3,0) lock may be thermally activated simply through density fluctuations, whereas the (4,1) lock involves a combination of density and dipole pair fluctuations. As is evident from Fig. 3, the rotational unlocking leaves the lattice unstrained, and so all processes of this type are *conservative.*

Obviously, in a random distribution of dimers, locks of all orders appear, and those with large signature values are expected to have long opening times with respect to slip motion. Thus, we do not expect these rotational lock-opening processes to significantly affect the estimate $\langle n \rangle = 5$ for the mean free "slip" length.

It should be emphasized here that if the dimers are frozen in below T_M, then a considerable heat of fusion is expected to be absorbed at the transition. Since, however, the cooperative rotational motions in the dimer system involve dislocation dipoles of rather small extent, the preservation of triangular symmetry, dynamically, should be readily attained in the low-temperature phase, so that the measured enthalpy change at T_M should be smaller than that predicted by the frozen-in model of disorder below T_M. An analogous system, which is dynamically disordered below T_M, is the rotator phase of paraffin, which will be discussed at length in Sec. VII.

It should be noted that any theory of the rotational motion of dimers which preserves the triangular lattice on a time average must include the coupling of the dimer motions to lattice vibrations and lattice shear defects. The simplest models incorporating phonon couplings are the compressible vertex models. These give rise to a first-order transition if the incompressible model has a critical heat-capacity exponent $\alpha > 0$. Although the present problem is more complex, due to the presence of shear defects we conclude that the transition, leading into the disordered dimer phase, is discontinuous if $\alpha > 0$ holds for the dimer system with steric coupling only, as considered in this paper.

III. NONCONSERVATIVE SLIP PROCESSES

It should be noted that at least two dimers must be involved in a rotational lock of the conservative type. The simplest nonconservative rotational unlocking process is shown in Fig. 4. In Fig. 4(a) the advancing dislocation 1^+ is blocked by the dimer shown as an ellipse, i. A dipole pair $(2^+,2^-)$ is created at P, and the barrier is removed from the path of 1^+ by the motion of 2^+ through at least one lattice spacing. The final unrelaxed position of the dimer is shown as the ellipse, f. In Fig. 4(b) the forward motion of 1^+ proceeds to the right, intersecting the common slip lines of 2^+ and 2^-. Owing to the torsion generated by this motion, the slip lines of 2^+ and 2^- are displaced with respect to each other by $\vec{b}$, the Burgers vector of 1^+. Thus 2^+ and 2^- may no longer annihilate one another. Instead, in their state of closest approach, they form an interstitial dipole. Apparently, no symmetrical

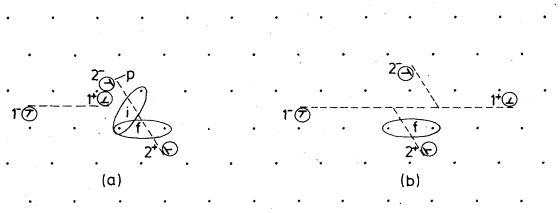

FIG. 4. Nonconservative rotational unlocking process for the impinging dislocation 1^+. The initial and final positions of the dimer, which is involved in blocking, are shown as the ellipses i and f, respectively. (a) shows the removal of the barrier through the creation of the dislocation dipole $(2^+,2^-)$ at P, and its separation; (b) shows the torsion created by the passage of 1^+, producing an interstitial dipole in the ground state. Lattice points are drawn in unrelaxed positions for the sake of simplicity.

process exists which can produce vacancy dipoles for this case.

In Fig. 5 we show the simplest barrier *translation* unlocking processes. These are all nonconservative. In step 1 the intermediate dipole, $(2^+,2^-)$, is created at P, and 2^+ or 2^- moves to its final position. In step 2 the torsion generated by the advance of 1^+ displaces the slip lines of 2^+ and 2^-, as is the case in Fig. 4. Here, however, vacancy dipoles are created in Figs. 5(a) and 5(c), whereas in Figs. 5(b) and 5(d) interstitial dipoles are generated. In these processes the minimum separation of $(2^+,2^-)$ is about one lattice spacing.

Note that in Figs. 4, 5(c), and 5(d) there is no possibility that another dimer moves into the blocking position upon separation of $(2^+,2^-)$. In the processes of Figs. 5(a) and 5(b), however, simple counting gives a probability, $q=\frac{1}{12}$ that this occurs. Thus we neglect this possibility in the following for the sake of simplicity.

There are roughly $\langle n\rangle^2$ possible configurations of the interstitial or vacancy dipoles for each of the processes shown in Figs. 4 and 5. Neglecting the elastic energy and assuming that the core energy for creation of the dipole is $2\gamma\mu b^2$, where μ is the Lamé shear constant, $\vec{b}$ is the Burgers vector, and γ is a constant factor less than 1, the probability $P(0)$ that a dislocation advances in the forward direction after being blocked scales as

$$P(0)\propto 5\langle n\rangle^2 e^{-2\beta\gamma\mu b^2}\,. \tag{1}$$

Up to this point we have only considered the simple picture where the dislocation 1^+ advances, leaving behind a pair $(2^+,2^-)$, which may take on approximately $\langle n\rangle^2$ configurations. If, however, we suppose, for instance, that 2^+ advances the slip and that one considers $(2^-,1^+)$ as the remnant pair, then a more complex degeneracy of states occurs. This is easy to see because the slip lines of 2^- and 1^+ are not parallel, so that their motions are not independent, due to the torsion generated when one crosses the slip line of the other. This effect is illustrated in Fig. 6 for the unlocking process of Fig. 4. Figures 6(a) and 6(b) are obtained as in Fig. 4. In Fig. 6(c), 2^- moves to the lower right crossing the original slip path of 1^+ and shifting it up as shown. Then in Fig. 6(d), 1^+ moves to the left followed by the motion of 2^- to the upper left. In Fig. 6(e), 1^+ moves to the right, and in Fig. 6(f), 2^- moves to the lower right. The result of these motions is that the pair $(1^+,2^-)$ wanders away from the original point of creation, so that an infinity of possible configurations of the pair may be reached, provided a member of

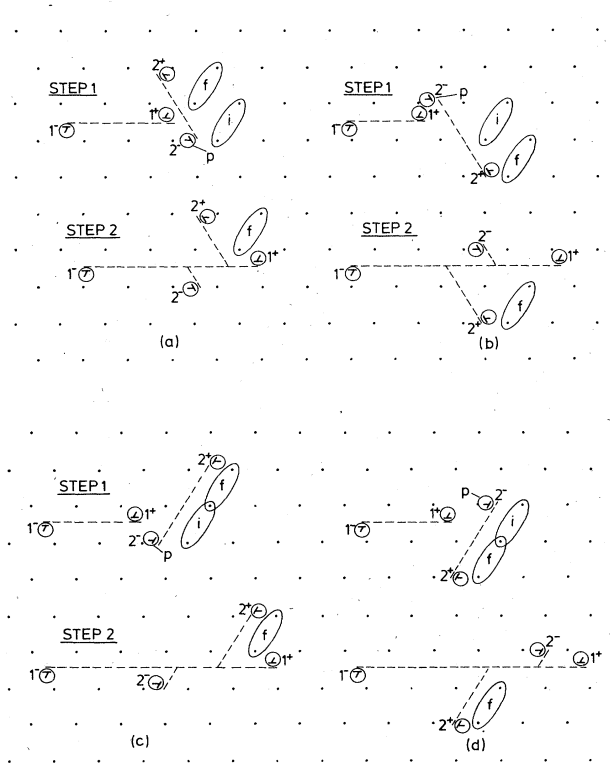

FIG. 5. Nonconservative translational unlocking processes for the impinging dislocation 1^+. The rotation is the same as in Fig. 4. (a) and (c) vacancy dipoles are created, whereas in (b) and (d) interstitial dipoles are generated.

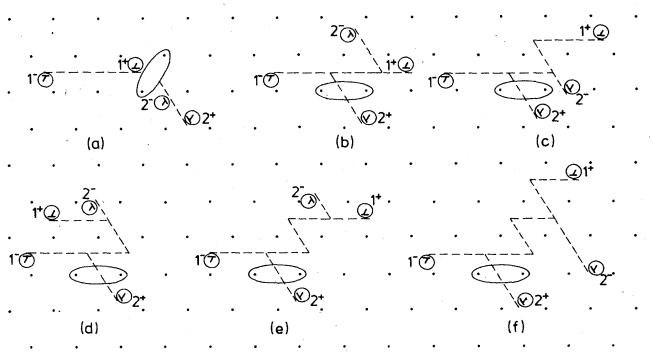

FIG. 6. Nonconservative rotational unlocking process for the impinging dislocation 1^+. (a) and (b) are the same as Fig. 4. Here, 2^+ is assumed to advance the slip, and the remnant pair is $(1^+,2^-)$. The noncommutative motions of 1^+ and 2^- in (b)—(f) (see text) produce an infinity of possible configurations for the pair.

the pair is not blocked. The configurations of Figs. 6(a), 6(b), and 6(c) may be surely realized and have the respective degeneracies $\langle n\rangle^2$, $2\langle n\rangle^2$, and $\langle n\rangle^2$. Assuming r is the probability that a new configuration with degeneracy $\langle n\rangle^2$ is produced through torsional slip-line crossing, then the average degeneracy for the pair $(1^+,2^-)$ in the process initiated in Fig. 6(a) is

$$\langle N\rangle = 4\langle n\rangle^2 + \langle n\rangle^2 \sum_{m=1}^{\infty} m r^m (1-r)$$
$$= \left[4+\frac{r}{1-r}\right]\langle n\rangle^2 . \quad (2)$$

Here we assume $r=$const, which should be true if $(1^+,2^-)$ is sufficiently far from the original blocking dimer.

In Figs. 7(a), 7(b), 7(c), and 7(d) we show the translational unlocking processes corresponding to Figs. 5(a), 5(b), 5(c), and 5(d), assuming that 2^+ advances the slip at angles $2\pi/3$, $-\pi/3$, $-2\pi/3$, and $\pi/3$ to the original slip line, respectively. Here, again, the remnant pair $(1^+,2^-)$ may take on an infinity of properly weighted configurations due to the torsion generated by the slip-line crossing effect. In Fig. 7 we show only the *third* step (to be taken after steps 1 and 2 of Fig. 5). It is easily seen that for each of these translational unlocking processes there are $\langle N\rangle$ possible configurations of the pair $(1^+,2^-)$ on the average, with $\langle N\rangle$ given in Eq. (2).

It should be noted that in the five nonconservative processes considered, in which the slip advances through kinks in the slip path with angles of $\pm\pi/3$ and $\pm 2\pi/3$, to the forward direction, the remnant pair $(1^+,2^-)$ has a resultant Burgers vector which may be of magnitude b or $\sqrt{3}b$. In the former case the remnant pair may fuse with the release of core energy $\sim\gamma\mu b^2$; in the latter, an unstable fused state may be created with the absorption of core energy $\sim\gamma\mu b^2$. In equilibrium both types of fused dislocations may be present.

In Figs. 8(a), 8(b), 8(c), 8(d), and 8(e), we show the fused dislocations (labeled 3) corresponding to the remnant pairs in Figs. 5(a), 5(b), 5(c), and 5(d), and 4, respectively. The slip line of the fused dislocation is shown (dotted-dashed line), the fused state being unstable in Fig. 8(d) only. In fact, if we exchange the roles of 2^+ and 2^- in these figures, then only in Fig. 8(d) is the fused state stable.

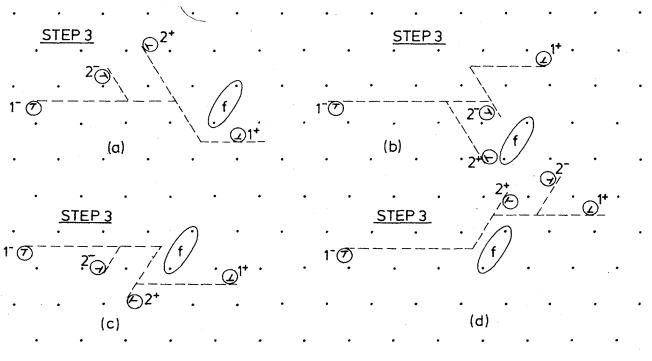

FIG. 7. Nonconservative translational unlocking processes in which the slip is assumed to advance through 2^+, and the remnant pair is $(1^+,2^-)$. (a)—(d) represent the third step in a continuation of the processes shown in Figs. 5(a)—5(d), respectively.

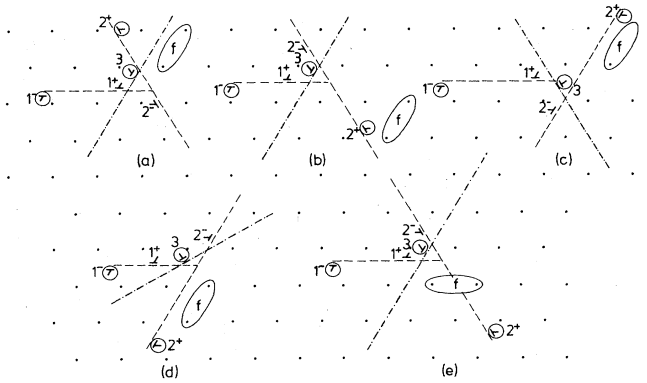

FIG. 8. Conservative barrier-bypassing processes through $(1^+,2^-)$-pair fusion. The fused dislocation is labeled 3, and its slipline is the dotted-dashed line. The configurations (a), (b), (c), (d), and (e) correspond to those shown in the first steps of the processes illustrated in Figs. 5(a), 5(b), 5(c), 5(d), and 4, respectively.

It may be seen that 3 in Fig. 8 is not blocked by the barrier which had impeded 1^+, shown again as the ellipse f. Thus 3 is free to move about $\langle n\rangle$ lattice spacings from its original position of fusion. Furthermore, the unstable fused state will be essentially pinned since the probability of encountering a blocking dimer at any point on its slip line is $\sim\frac{1}{2}$.

It may be seen from Fig. 8 that the combined motion of 2^+ and 3 produces branching of the original slip line in any of the four symmetry directions lying obliquely to it. Although such fusion-type barrier-bypassing processes are simple and have the lowest activation energy of all the processes we have considered, we believe that the entropy generated in the pair configurations will contribute most of the entropy necessary for melting. Furthermore, the unstable fused state contributes essentially no entropy and readily decays into its constituents.

In the following sections we consider a model of dimer melting in which we neglect the effect of fusion and branching. Furthermore, we neglect the differences, discussed at length above, in the configurational degeneracies of the remnant pairs, associated with nonconservative slip in the various crystallographic directions. Finally, we neglect the intricate effects of torsional wandering.

In our model we consider the slip paths to be random walks on a triangular lattice of equal step length $\langle n\rangle l_0$, l_0 being the lattice constant. Furthermore, we consider the remnant pairs to be generated at, and to remain rather close to, each step position on a given path, so that the pairs may be labeled by these positions. Finally, we attribute to every remnant pair a certain average configurational degeneracy. In spite of the complicated nature of

dislocation dissociation in a dimer solid, it is hoped that our model contains the essential physical features of processes discussed in this section.

IV. SCREENING THEORY OF DIMER MELTING

A. General discussion

In this section we assume that the energy of a slip line in the dimer solid may be written as[12,14]

$$E(\vec{r}_0,\vec{r}_N,\mathscr{C})\cong\frac{2\gamma\mu b^2}{l_0\langle n\rangle}\int_{\mathscr{C}}dS+\mu b^2[2\pi(1-\nu)]^{-1}\times\int_{R_0'}^{|\vec{r}_N-\vec{R}_0'|}[\epsilon_{\rm as}(r')r']^{-1}dr' , \tag{3}$$

where l_0 is the lattice spacing, μ and ν the continuum elastic Lamé constants, b the magnitude of the Burgers vectors of a reference pair, whose elements lie at the endpoints of the slip path $\mathscr{C}$ at $(\vec{r}_0,\vec{r}_N)$, $\langle n\rangle$ the average length of a slip segment, R_0' the core radius, and γ the core-energy parameter ($0.01\lesssim\gamma\lesssim0.1$).

The first term represents the core energy in which all Burgers vectors are taken of equal magnitude, b. The second term represents the elastic interaction energy of the endpoints of $\mathscr{C}$, where the only effect of the remnant pairs which dress $\mathscr{C}$ is considered to be a screening or antiscreening of this interaction energy. The usual logarithmic expression is obtained when the screening or antiscreening function $\epsilon_{\rm as}(r')$ is set equal to a constant. As we shall see in the following section this expression for the elastic energy should perhaps be modified because the mutual interaction of all dislocation pairs may lead to an additional *line* energy for the slip path which must be combined with the core energy given in Eq. (3).

Since the usual melting criterion[12] for two-dimensional solids is based upon the dissociation of a widely separated reference pair, melting will only occur, if the gain in entropy more than compensates for the increase in energy given in Eq. (3), as the path length $N\langle l_0\rangle$ increases. Here, N is the number of steps on the slip path connecting the reference pair. The increase in entropy in our model derives from (a) the increase in the possible number of slip paths connecting the reference pair, and (b) the increase in the total number of possible remnant-pair configurations. In subsection B we obtain an upper bound T_M^* on the melting temperature, based solely on the first entropy source. In subsection C the configurational entropy of the pairs is added to the model to obtain the upper bound T_M^{**}.

B. Melting criterion without remnant-pair entropy

In this section, melting is considered to derive from the increase in the number of slip paths available to a dissociating reference pair. For a path of length L, the number of steps is roughly $N=L/l_0\langle n\rangle$. Taking this path to be a *random* walk of N equal steps, the probability $p(m)$ of arriving at $m=|\vec{r}_N-\vec{r}_0|(l_0\langle n\rangle)^{-1}$ steps from an origin at $\vec{r}_0$ is

$$p(m)\cong(\pi N)^{-1}e^{-m^2/N} . \tag{4}$$

If, on the triangular lattice, z_0 is equal to the five possible directions that may be taken at each step, the total number of paths of length L is z_0^N, giving $z_0^N p(r)$ paths $\mathscr{C}(r_0,r_N)$ of length L. Taking $\epsilon_{\rm as}(r')=$const in Eq. (3), the partition function of the single random slip path may be written approximately as

$$Z=\sum_{\{\vec{r}_N\}}\sum_{\{\mathscr{C}(\vec{r}_0,\vec{r}_N)\}}e^{-\beta E(\vec{r}_0,\vec{r}_N,\mathscr{C})} \tag{5a}$$

$$\simeq R_0\int_{R_0}^{\infty}dr\left[\frac{r}{R_0}\right]^{(1-3\beta T_M^{\rm as})}I(r) , \tag{5b}$$

where

$$I(r)\equiv\pi^{-1}\int_0^{\infty}dL\,L^{-1}e^{-(\gamma' L+r^2L^{-1})}$$
$$=\pi^{-1}\left[K_0[2r(\gamma')^{1/2}]-\frac{1}{r(\gamma')^{1/2}}K_1[2r(\gamma')^{1/2}]+K_2[2r(\gamma')^{1/2}]\right]\quad\text{for Re}\gamma'>0 , \tag{5c}$$

with $\gamma'\equiv2\beta\gamma\mu b^2-\ln z_0$, $R_0\equiv R_0'(l_0\langle n\rangle)^{-1}$, and

$$k_B T_M^{\rm as}\equiv\mu b^2[6\pi(1-\nu)\epsilon_{\rm as}]^{-1} , \tag{5d}$$

where $K_i(z)$ is a Bessel function of ith order. The stability of the solid phase requires that Z be finite, so that a *necessary* condition for stability is $\text{Re}\gamma'>0$, or $T_M\le T_M^*$ with

$$K_B T_M^*=\frac{2\gamma\mu b^2}{\ln z_0} . \tag{6}$$

For $\text{Re}\gamma'<0$ the slip line grows in length without bound. If, however, the elastic energy of the endpoints greatly exceeds that of the core energy of the line, one expects that the endpoint separation may remain finite while $L\to\infty$. In the present context this limit is obtained when

$$T_M^*\ll T_M^{\rm as} , \tag{7}$$

where $T_M^{\rm as}$ is given by Eq. (5d). In such a case interaction effects of slip-line crossing not considered in this paper must be introduced into the theory, and the melting criterion $T_M\le T_M^*$ will be altered. For instance, such crossings may very well lead to a repulsive interaction of the excluded-volume type, which requires a modification of Eq. (4).

It may be worthwhile to point out that for the monatomic solid, one must use, instead of Eq. 5(c), $I(r)=r^{-1}e^{-\beta(2\gamma\mu b^2)}$, since the slip is *linear* and thus *conservative* in that case. This implies a reduction of the phase space by a factor r^{-1}. For such a system the only entropy term arises from the configurations of the slip-line endpoints, a quantity that is independent of the relative separation of these points. Thus one obtains, from the analog of Eqs. (5), in the case of a monatomic solid, the condition $T_M\le3T_1$, where

$$k_B T_1=\mu b^2[6\pi(1-\nu)\epsilon]^{-1} . \tag{8}$$

Here, $\epsilon(T) \geq 1$ is the dielastic constant of the monatomic solid, derived from thermally produced dislocation dipoles, which is as yet unconsidered in the derivation of Eq. (6).

In most theories of monatomic melting, one uses the finiteness of the polarizability, instead of Z, as the stability criterion. This leads to the condition $T_M \leq T_1$, which may be more appropriate than $T_M \leq 3T_1$, derived above. Note that when the time scale of conservative lock-opening processes, discussed in Sec. II, approaches that of gliding motion, then $T_M^* \rightarrow T_1$ from above, within the approximations made in this section. Such a limit may be appropriate in the short-chain systems, where rotational motion may be quick, and is again discussed in Sec. VII in a tentative interpretation of the phase diagram of phospholipid bilayers as suggested by Fig. 10.

Comparison of Eqs. (8) and (6) clearly indicates the difference within our model between monatomic and dimer dislocation melting in two dimensions. In the former case the elastic energy competes with the configurational entropy of the reference pair to produce the transition, whereas in the latter it is the competition between a line energy, associated with the cores of the remnant pairs, and their configurational entropy which leads to a transition. We return to this point in Sec. V, where we argue that the mutual elastic interaction of the dressed slip line may provide a further line energy of elastic origin for large N, leading to the definition of an effective line-energy parameter γ_{eff}.

C. Melting criterion including remnant-pair entropy

If Eq. (6) yields roughly the order of magnitude of T_M, then the thermal energy near the melting transition is roughly $\gamma\mu b^2$, the core energy needed to dissociate any stable fused pair. To estimate the effect on T_M^* of the degeneracies expected for excited pairs, as discussed at length in Secs. II and III, we assign to each pair a configurational degeneracy $z^* \equiv \text{const}$, which represents some average value of the degeneracies enumerated in Sec. III. In this approximation the partition function is of the same form as that given in Eqs. (5), with the simple replacement $z_0 \rightarrow z_0 z^*$. Thus the upper-bound melting temperature becomes

$$T_M^* = \frac{2\gamma\mu b^2}{\ln(z_0 z^*)} \ . \tag{6'}$$

V. MUTUAL INTERACTION ENERGY OF A DRESSED SLIP LINE

The elastic interaction energy is represented in Sec. IV as $W_0(N) = \text{const} \times \ln N$ for large N, where the effect of the remnant pairs is expressed as a screening (or antiscreening) of the elastic medium through the introduction of ϵ_{as}. An alternative approach is to include the mutual interaction of all the dislocations, associated with a given slip line of N steps,[14]

$$W(N) = -\mu b^2[2\pi(1-\nu)]^{-1} \times \sum_{m=0}^{M} \sum_{l>m}^{M} [\cos(\phi_m - \phi_l)\ln S_{ml} + \sin(\phi_m - \phi_{ml})\sin(\phi_l - \theta_{ml})] \ . \tag{9}$$

Here, m labels the $M = 2N$ dislocations, dressing the path at the positions $\{\vec{r}_m\}$. The Burgers vectors are taken to be $\{\vec{b}_m \equiv b\vec{B}_m\}$ with $\{B_m = 1\}$, and the core radius $R_0' \sim b$. The relative positions are defined by $\vec{S}_{ml} \equiv b^{-1}(\vec{r}_m - \vec{r}_l)$, and (ϕ_m, θ_{ml}) are the angles that $(\vec{B}_m, \vec{S}_{ml})$ makes with respect to the x axis of a coordinate system, fixed in the lattice plane. Note that Eq. (9) does not take the torsional and curvature effects produced by the slip into account. This would require a rather difficult calculation of the geometry of the lattice. This neglect is probably most severe in the liquid phase, since collective states of dislocations, like grain boundaries and disclinations are only correctly calculated if torsion and curvature is accounted for. In that case it is the second term of Eq. (9) which apparently stabilizes orientational order in the liquid.

For the numerical work discussed presently, random walks were generated on a triangular lattice of lattice constant $5b$, and the average value of $W(N)$ computed for 30 paths of given N, using Eq. (9). The reference pair is located at $(\vec{r}_0, \vec{r}_N)$ with $\vec{B}_0 = -\vec{B}_N = \hat{x}$. Furthermore, we have assumed that each remnant pair is well localized and can be assigned to a particular lattice point $\{\vec{r}_p; 1 \leq p \leq N-1\}$ along the path. This allows us to label these dislocations with $m \equiv (p,\sigma)$, σ being ± 1: The dislocation (p,σ) is located at $\vec{r}_p$ on the slip segment $\sigma(\vec{r}_{m+\sigma} - \vec{r}_m)$, and as can be seen from the figures of Sec. III, $\vec{B}_{(p,-1)} = -\vec{B}_{(p-1,1)}$. Furthermore, we take a random choice for $\vec{B}_{(p,1)}$ between the two values $\pm(5b)^{-1}(\vec{r}_{p+1} - \vec{r}_p)$. In Fig. 9 the normalizing constant is $W_e \equiv \mu b^2[2\pi(1-\nu)]^{-1}$. In computing $W(N)$, we have taken the constituents of each remnant pair to have Burgers vector $\vec{b}$ and a mutual separation of one lattice spacing. At such small separations the elastic interactions within a pair are essentially of core type with energies $3\gamma\mu b^2$ or $\gamma\mu b^2$, depending on the relative orientation of the constituent Burgers vectors. Therefore, *on the average,* for a sufficiently long random walk, the core energy is $2\gamma\mu_b^2$ per pair or $\gamma\mu b^2$ per dislocation. Consistent with this fact we drop all terms in $W(N)$ which involve interactions within a pair.

Although we obtain considerable scatter in $W(N)$, as shown by the error bars in Fig. 9, it is evident that the assumption of a constant ϵ_{as} is invalid. In fact, it seems that in no region of N is the logarithmic law applicable as representing the mutual interaction energy of the slip line. Above $N = 120$ this interaction energy appears to become linear with increasing N, implying $\epsilon_{\text{as}}(r) \simeq \frac{1}{2} r^{-1} l_0 \langle n \rangle S$ + const, where S is the slope of the curve plotted in Fig. 9 for large N. However, other dependencies are also possible, such as an oscillatory behavior of $\epsilon_{\text{as}}(r)$, leading eventually to a constant envelope ϵ_{as}.

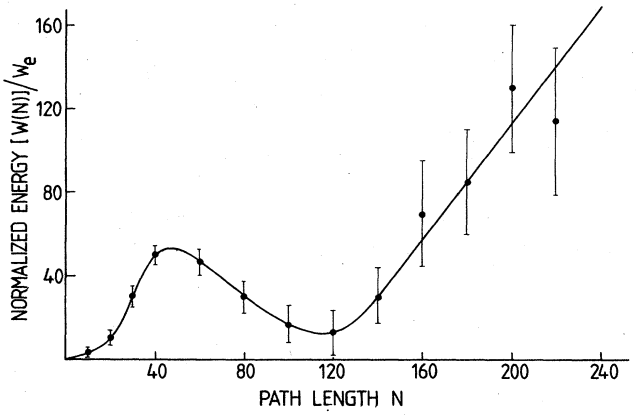

FIG. 9. Normalized elastic mutual interaction energy of a dislocation-dressed random slip path versus number of steps on the path, averaged over 30 paths of given length (solid curve). Error bars indicate root-mean-square deviations from the average values shown as solid circles.

Note that ϵ_{as} does not have the same physical significance as the dielastic function $\epsilon_d(T) \geq 1$, because this would imply that each pair formed at a kink of the slip path is relaxed in such a way as to minimize the overall strain energy. Furthermore, no thermal average was made, due to computer-time restrictions, so that ϵ_{as} is temperature independent.

If we accept the linearity of $W(N)$ for large N, then, since we have calculated $W(N)$ assuming the presence of a single dressed slip line, one must account for the presence of additional thermally produced dipole pairs through the replacement $S \rightarrow S\epsilon_d^{-1}(T)$. Thus the calculations of Sec. IV would then be altered by the replacement

$$\gamma \rightarrow \gamma_{\text{eff}} \equiv \gamma + S\epsilon_d^{-1}(T)[2\pi(1-\nu)]^{-1} , \tag{10}$$

so that the upper-bound melting temperature [see Eq. (6′)] would become, in that case,

$$k_B T_M^* = 2\mu b^2 \{\gamma + [2\pi(1-\nu)\epsilon_d(T)]^{-1} S\} [\ln(z_0 z^*)]^{-1} . \tag{11}$$

VI. COMPARISON OF DIMER AND MONATOMIC MELTING IN TWO DIMENSIONS

Clearly, the steric constraints on the dimer solid make this system more reluctant to melt than its monatomic counterpart. As discussed in Sec. IV the monatomic solid will melt, according to Eq. (7), below

$$k_B T_1 = \mu b^2 [6\pi(1-\nu)\epsilon_b(T_1)]^{-1} ,$$

where the dielastic constant ϵ_b characterizes the elastic polarizations, without the constraint of dimerization. On the other hand, if one construes a *fictitious* monatomic solid in which the dimers are replaced by large atoms with diameters corresponding to the dimer length, the lattice constant increases by a factor $\sqrt{2}$ over that of the dimer lattice. This implies an upper-bound melting temperature

$$k_B T_2 = 2\mu b^2 [6\pi(1-\nu)\epsilon_{\sqrt{2}b}(T_2)]^{-1} .$$

Obviously, $T_2 > T_M^*$, since the entropy-producing degrees of rotational freedom are supressed. Therefore, the condition $T_1 < T_M^*$ may be explicitly written as

$$1 < A < [2\epsilon_b(T_1)/\epsilon_{\sqrt{2}b}(T_2)] , \tag{12a}$$

with

$$A \equiv 3\epsilon_b(T_1)[4\pi(1-\nu)\gamma + S\epsilon_d^{-1}(T_M^*)][\ln(z_0 z^*)]^{-1} . \tag{12b}$$

For a rough estimate we take $\epsilon_{\sqrt{2}b} = \epsilon_b = \epsilon_d = 1$, $\nu = 0.5$, $S = 1.30$, $z_0 = 5$, and $0.01 \leq \gamma \leq 0.1$. Taking $z^* = \langle n \rangle^2$ with $\langle n \rangle = 5$, we obtain $0.85 < A < 1.20$, which violates Eq. (12a) only slightly at the lower limit. Note that in writing Eqs. (12) we have assumed that the Lamé constants are the same for the three systems considered. This may hold since long-wavelength properties should not be sensitive to the atomic structure.

In the case of a small core-energy parameter γ, the dimer barriers are easily overcome, and near T_M this leads to a large thermal production of vacancy and interstitial remnant pairs. Once a sufficient number of these is available, the blocking dimers may be avoided through climb processes, which have not been considered in this paper. Thus, for small γ, the constraint of dimerization is relaxed, and we expect that the upper-bound melting temperature of the dimer solid approaches that of its monatomic counterpart: $A \rightarrow 1$ as $\gamma \rightarrow 0$. In that case one obtains $T_M^{as} \rightarrow T_1$, as was discussed in the context of Eq. (7). Such a limit is not very realistic since a vanishing core energy $\gamma \rightarrow 0$ also implies $\mu \rightarrow 0$.

On the other hand, if the core-energy parameter becomes exceptionally large so that $A > 2$, we attribute the breakdown of our model to the fact that the cooperative lock-opening mechanisms discussed in Sec. II become important and determine the time scale of the dislocation glide motion. For the parameters used, this will occur for $\gamma \gtrsim 0.5$.

Our final remarks in this section are addressed to the order of the melting transition. Within the model of random slip paths a continuous transition will be predicted, even if excluded-volume effects are incorporated. In addition to the lattice-coupling effects discussed above, there is an additional effect which can drive the transition first order: From the qualitative discussion in Secs. II and III, one sees that there is an inherent source of instability of the slip line with respect to branching. Although we have only begun to study this problem analytically, we intuitively feel that this branching instability could be the principal driving mechanism for the observed discontinuous transition at T_M.

VII. THREE-DIMENSIONAL EXTENSIONS OF THE MODEL: CHAIN FLEXIBILITY

So far we have confined ourselves to the purely two-dimensional aspects of the melting of a lipid monolayer. If one assumes that the CH_2 chains remain rigid during the melting process, the finite thickness d of the layer

(roughly the length of the extended chains, if we neglect the tilting angle of the molecules) may be taken into account by writing $T'_M = T_M d/d_0$, where T_M is the melting temperature of the two-dimensional system, and $d < d_0$. Here, d_0 is the monolayer thickness where deviations from two-dimensional behavior are observed. This is a consequence of the fact that the dislocation cores pierce straight through the layer due to the assumed rigidity of the chains for $d < d_0$.

Thus, in the approximation of rigid chains, we expect the internal energy of the dislocation system to be proportional to d, and the entropy change upon melting, $\Delta S'_M = \Delta S_M$, assumes its two-dimensional value. Then the latent heat of melting is expected to be proportional to d: $\Delta Q \equiv T'_M \Delta S'_M = (T_M \Delta S_M) d$.

The experimental melting curve and latent heat of melting is shown in Fig. 10 as a function of CH_2-chain length. Clearly, the rigid-chain behavior is observed for the short-chain homologs. For short chains we expect the constraint of dimerization to be strongly felt, so that the two-dimensional aspects of melting should be dominant. (We address ourselves to the apparent instability of the short-chain limit, suggested by the dashed line in Fig. 10, in the following paragraphs.)

With increasing d, however, jogging of the CH_2 chains as a result of the trans-gauche isomerizations occurs with increasing ease at the free ends of the chains. This leads to the production of screw-type dislocation cores within the layer, running parallel to the layer surface. Therefore, as the chains become more flexible, dislocation loops are generated. The vertical portions of these loops (segments parallel to the chain axis) are of the edge type, representing the extensions of the point dislocations discussed above. This leads to a convex shape for the melting curve as a function of d, as has been shown for the case of paraffin.[10,15] Paraffin is a multilayered system in which the lamellae are composed of CH_2 chains, orientated relative to the lamellar surfaces in a fashion similar to that found in lipid bilayer systems.

Note that the rotator phase observed in paraffin,[10] a consequence of the anisotropic shape of the polymer chains, precedes melting and is analogous to the low-temperature dynamically disordered state of the dimers considered in this paper. As pointed out earlier, in both cases a triangular lattice structure is maintained.

The CH_2 chains in paraffin, however, are not subject to dimerization. For the thicker lipid membranes, this constraint is expected to decrease in importance. In fact, the experimental melting curve seems to indicate convexity for CH_2 chains of more than 20 units, although more experimental data are needed to make a conclusive statement.

The reason for the convexity of $T'_M(d)$ is simple to understand: The dislocation loops, which can form when the chains become flexible, increase the entropy of the dislocation system, decreasing $T'_M(d)$ from the value expected on the basis of rigid chains and straight edge dislocations. Assuming for simplicity that the departure from linearity beginning at d_0 may be expressed as

$$T'_M \cong T_M d_0^{-1} d(1-\alpha_1\delta) ,$$

where $\delta = (d-d_0)/d_0 \ll 1$, and that $\Delta S'_M \cong \Delta S_M(1+\alpha_2\delta)$ in the same range of d, one obtains

$$\Delta Q \cong T_M \Delta S_M d_0^{-1} d[1+(\alpha_2-\alpha_1)\delta-\alpha_1\alpha_2\delta^2] . \quad (13)$$

Since $\Delta Q(d)$ in Fig. 10 appears linear, even beyond the point where $T'_M(d)$ becomes convex, we conclude that $\alpha_1 \approx \alpha_2$. It remains for experiment to verify the predicted convex shape of $\Delta Q(d)$ for larger values of d, which should have a considerably weaker curvature than that of $T'_M(d)$.

Extrapolating the ΔQ curve of Fig. 10 linearly to the left (see dashed line) shows that, below $N_0 = 8$ CH_2 units, $\Delta Q < 0$ is obtained. Such behavior cannot be explained by our present model. It is possible that for $N \gtrsim N_0^*$, where N_0^* is some chain length greater than N_0, the dynamical disordering of the dimers and melting occurs simultaneously. In paraffins there is evidence that the rotator phase becomes unstable below T'_M for sufficiently large N,[10] giving support to the above conjecture.

Another explanation of the unphysical instability for $N < N_0$ is that the melting transition becomes continuous for such short chains. This possibility arises if the rotational fluctuations of the dimers are so rapid that the conservative lock-opening processes discussed in Sec. II allow the formation of straight slip paths. Under the assumption that only conservative glide processes contribute to the dissociation of dislocation pairs, a continuous transition is possible for two-dimensional systems.

Finally, the problem may also be connected with the fact that for increasing N, screw dislocations form through chain jogging which are not contained in the present two-dimensional dimer model. Since these are intimately related to the liquid-state properties of the system above T'_M for systems consisting of long-chain molecules,[16] the anomaly at $N = N_0$ may signify a transition driven by screw dislocations at larger N.

We would like to emphasize that the dislocation-loop—dissociation viewpoint of melting, applied to lipid membranes, would offer a unified approach for treating the simultaneous loss of triangular symmetry in the membrane surface and the "chain melting" within the mem-

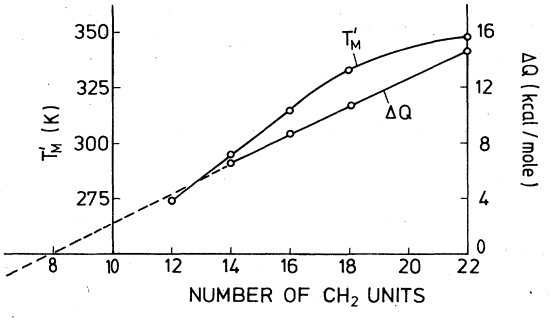

FIG. 10. Melting temperature and latent heat versus CH_2-chain length for lecithin-water mixtures, a lipid monolayer system (see Ref. 2). The dashed line is an interpolation of the ΔQ data.

brane bulk. This approach is very advantageous when considering the transition between short- and long-chain behavior, as has been amply demonstrated in the theory of paraffin melting. In fact, as can be concluded from the smoothness of $T'_M(d)$ in Fig. 10, and the fact that chain order and triangular order disappear simultaneously at T'_M, the melting mechanism cannot be separated into a chain-disordering process and a surface-dimer-disordering process.

With regard to the paraffin analogy, it has been conjectured[10,16] that liquid paraffin may be describable as a smectic-A liquid crystal. In order that curvature-type elastic laws of a general nature be obeyed in lamellae consisting of long molecules, screw dislocations must be present with Burgers vectors parallel to the molecular axis.[16] Thus, surface roughening must occur in such systems. In fact, drilling motions of the long molecules through the layer surfaces has been discussed at length for the case of paraffin.[10] Whether or not such effects are important for lipid membranes depends on the stabilizing effect of the polar heads, which so far have not been included in the model developed here.

ACKNOWLEDGMENTS

This work has been supported in part by North Atlantic Treaty Organization (NATO) Research Grant No. 028.82, and by the Wissenschaftliche Gesellschaft des Saarlandes (West Germany).

[1]J. F. Nagle, Ann. Rev. Phys. Chem. **31**, 157 (1980), which contains a review of recent theoretical work.
[2]A. Caille, D. A. Pink, F. de Verteuil, and M. J. Zuckermann, Can. J. Phys. **58**, 581 (1980).
[3]M. J. Zuckermann, D. A. Pink, M. Costas, and B. C. Sanctuary, J. Chem. Phys. **76**, 4206 (1982).
[4]M. Tessier-Lavigne, A. Boothroyd, M. J. Zuckermann, and D. A. Pink, J. Chem. Phys. **76**, 4587 (1982).
[5]D. Pink, T. J. Green, and D. Chapman, Biochemistry J. **19**, 345 (1980).
[6]O. G. Mouritsen, A. Boothroyd, R. Harris, N. Jan, T. Lookman, L. MacDonald, D. A. Pink, and M. J. Zuckermann, J. Chem. Phys. **79**, 2027 (1983).
[7]A. Caille, A. Rapini, M. J. Zuckermann, and A. Cros, Can. J. Phys. **56**, 348 (1978).
[8]S. Doniach, J. Chem. Phys. **68**, 4912 (1978).
[9]D. Marsh, J. Membr. Biol. **78**, 145 (1974).
[10]A. Holz, J. Naghizadeh, and D. T. Vigren, Phys. Rev. B **27**, 512 (1983).
[11]D. Kuhlmann-Wilsdorf, Phys. Rev. A **140**, 1599 (1965).
[12]J. M. Kosterlitz and D. J. Thouless, J. Phys. C **6**, 1181 (1973).
[13]A. Holz and J. T. N. Medeiros, Phys. Rev. B **17**, 1161 (1978).
[14]F. R. N. Nabarro, Adv. Phys. **1**, 271 (1952).
[15]D. T. Vigren, Phys. Rev. B **27**, 2932 (1983).
[16]A. Holz, Phys. Lett. **96A**, 475 (1983).